Acta Materialia Transylvanica 8/2. (2025) 55–59.
DOI: Hungarian: https://doi.org/10.33923/amt-2025-02-02
English: https://doi.org/10.33924/amt-2025-02-02

ACTA MATERIALIA TRANSYLVANICA

Effect of Laser Welding Parameters on the Microstructure of Lath-martensitic Thin Steel Plates

Enikő Réka FÁBIÁN

Óbuda University, Bánki Donát Faculty of Mechanical and Safety Engineering, Institute of Materials and Manufacturing Sciences, Department of Material Technology. Budapest, Hungary, fabian.reka@bgk.uni-obuda.hu

Abstract

In this study lath martensitic microstructure in S235JR and Mn-B alloyed steel sheets were produced. The Mn-B steel used as A and B pilar at autocars Laser welded blanks are an innovative way for automakers to reduce the weight of their vehicles while improving safety at the same time. We created welded joints with different parameters. Welding with 4100mm/min speed the weld metal hardness is similar to the late martensitic base material, and only a narrow heat affected zone is softened. Welding with lower speeds resulted softening of the weld metal and a double heat-affected zone: hard next to the weld metal and soft outside it.

Keywords*: lath martensite, laser welding, hardness.*

1. Introduction

The characteristics of the martensitic microstructure of steels depend on the carbon content of the steel. According to Krauss [1], during hardening, if the carbon content is below 0.6%, lath martensite is formed in the microstructure. Between 0.6% and 1%, we can speak of a mixed microstructure, which becomes increasingly plate-like rather than lath-like as the carbon content increases. With a carbon content above 1%, plate martensite is obtained. Literature data show that lath martensite appears below a carbon content of 0.6%, but below 0.3% C, this structure appears purely as a result of rapid cooling from the austenitic state [2, 3]. The lath martensite has a characteristic multilevel microstructure. The lath martensite is formed in parallel of parquet- or lath-like crystallites called laths.

Lath martensite consists of parallel laths, which are crystallites. Lath martensite characteristicaly has a multi-level microstructure. The transforming austenite contains several bundles. Each bundle consists of blocks bounded by large-angle grain boundaries, which in turn are formed by lamellae [4]. Numerous articles have been published in recent years on the formation and crystallographic analysis of lath martensite microstructures [5, 6]. As the C content increases, the structure of the blocks and bundles becomes finer [7, 8]. Depending on the carbon and alloying elements content researchers have created lath martensite by rapid cooling from high temperatures [7, 8, 9, 10].

The lower the carbon content of the steel, the higher the austenitizing temperature and the faster the cooling rate must be in order to create a pure martensitic structure [9, 10]. According to literature data [11] commercial hot-rolled high strength steel plates microalloyed with boron (C = 0.25%, Mn = 1.20%, B=0,006%), after austenitization at 950 °C, can form nearly 100% martensite by cooling at a rate of 100 °C/s, and nearly 71% martensite and 29% ferrite at a cooling rate of 50 °C/s. In another series of experiments, Morito et al [12] have produced lath martensitic microstructure at high-nickel and cobalt alloyed maraging steel and at two boron-microalloyed steels with very low carbon content. All three steels were cooled in brine from an austenitizing temperature of 1200 °C.

In the automotive industry, boron- and manganese-alloyed, press-hardened martensitic steels are used to form A and B pillars [13]. Martensite with a lath structure can support significant deformation [14]. The automotive industry aims to intro-

duce laser welding joints in high-strength steels in order to save material [15]. There is no data in the literature on what happens to the martensitic structure formed by press hardening during laser welding.

2. Experimental materials, experimental background

For the experiments, we used S235JR and PHS®1500 press-hardened steel (branded Usibor®1500 by Acelor Mital) commonly used in the automotive industry. According to the manufacturer's data sheet, the chemical composition of the PHS®1500 steel is: C=0.22%, Mn=1.3%, B=0.0035%, Si=0.25% [16].

Before heat treatment, the coating layer on the surface of the PHS 1500 steel sheet was removed. The samples were then austenitized in a laboratory furnace at a temperature of 1100 °C and then quenched in ice water. The microstructure of the samples after quenching is shown in Fig. 1. The average hardness of the unalloyed steel sheet with lower carbon content was 293HV1, while the hardness of the Mn-B alloyed sample was 450 HV1 after heat treatment.

After fitting the heat-treated samples together, we welded them using a Trump TLF 5000 turbo CO2 device. The technological data set for the test is shown in Table 1. The welding parameters described here were determined based on empirical data. Due to the reduction in welding speed, the focus spot position had to be adjusted in order to achieve a properly penetrated weld.

Table 1. *Welding data*

Nr.	Power (W)	Method	Speed (mm/min)	Focus position (mm)
I	5000	CW	4100	0
II	5000	CW	2500	+5
III	5000	CW	1300	+7.5
IV	5000	CW	1050	+10

Metallographic polishes were prepared from the samples. Cutting was performed on a metallographic cutting machine with water cooling. The cross-section samples were prepared using traditional metallographic methods and then examined using a Keyence VHX-2000E light microscope. After the light microscopic examination, ultrasonic hardness measurements were performed on the samples. The hardness measurements were performed using a Krautkramer Branson Microdur II device. The load force was 1 kg in all cases. We measured the change in hardness on the samples near the crown surface so that in each case the measurement range was: base material - heat-affected zone - weld metal - heat-affected zone - base metal.

3. Test results

In the case of Mn-B alloy steel, the welds were formed across the entire cross-section of the plate under the parameters used. In the case of Mn-B alloy steel, the laser technology parameters shown in Table 1 resulted in good through welds. No significant porosity or cracks were observed (Fig. 2), despite the fact that the base material is highly resistant and a high-hardness microstructure formed either in the weld or in the heat-affected

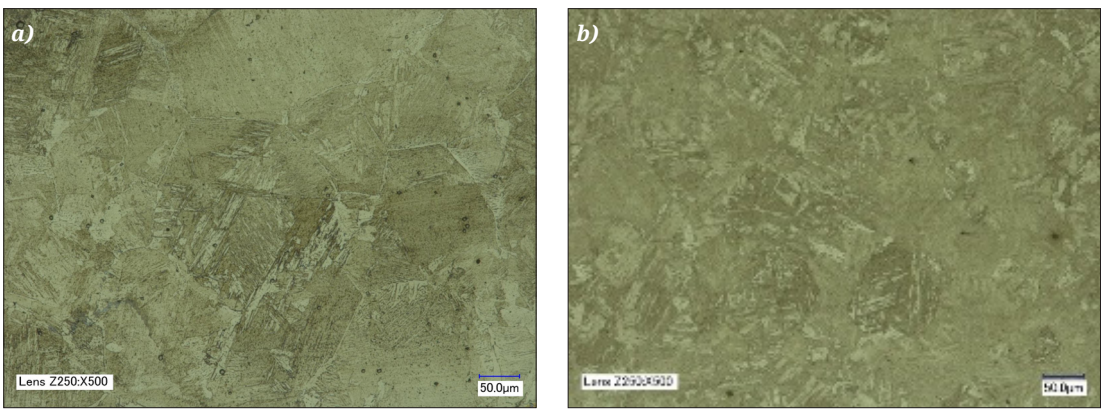

Fig. 1. *Microstructure of heat-treated steels: a) S235, b) Mn-B alloyed steel.*

zone, as can be seen in Fig. 3 which shows the hardness measurement results.

According to the hardness measurement results, when welding was effectuated at a speed of 4100 mm/min, the hardness of the weld metal, which is barely more than 1 mm wide, is equal to the hardness of the lath martensitic base material. Hardness decreased to 310–330 HV1 in the very narrow heat-affected. When welding at a speed of 2500 mm/min, the hardness decreased to 310 HV1 in the center line of the weld metal and in the narrow heat-affected zone, while the weld metal is characterized by a hardness above 400 HV1, despite the fact that the grain boundaries of the weld metal are ferritic (Fig. 4). In the central 0.8 mm zone of the weld metal of sample III, the hardness varied between 250 and 290 HV1, followed by a 0.7 mm high-hardness (470-500 HV1) heat-affected zone and a narrow 310 HV1 heat-treated zone.

Welding at 1050 mm/minute resulted in the lowest hardness (240-270 HV1) weld metal, which was 1.8 mm wide, with a 0.5 mm heat-affected zone with a hardness above 400HV1, outside of which the hardness fell below 300HV1 in a narrow range.

Although in the case of boron micro-alloyed steel the hardnesses reached 500 HV1 in some places, we did not find any cracks in any of the samples. A possible explanation for this favorable property in terms of crack formation is the cubic lattice structure [17]. due to low carbon content.

Literature data show that in boron-micro-alloyed steels, the boron segregation can cause grain boundary cracks [18]. If the cooling rate is high, boron segregation does not appear

Welding of martensitic low-carbon unalloyed steel plate samples according to the data in Table 1, shows that even at a welding speed of 4100 mm/min, a narrow continuous, full-penetrated weld was formed, as can be seen in the images in Fig. 5 When the highest welding speed was used, the hardness of the weld metal was the same as that of the martensitic base material, followed by a narrow (~0.3 mm wide) softened heat-affected zone, as shown in Fig. 6.

At a welding speed of 2500 mm/min the weld metal achieved a hardness of 240–250 HV, in the range of 0.2–0.3 mm, it reaches the characteristic hardness of martensitic base material, followed by slight softening in the narrow heat-affected zone.

At a welding speed of 1300 mm/min, the characteristic hardness of the weld metal and heat-affected zone was around 200 HV1, with one or two outliers.

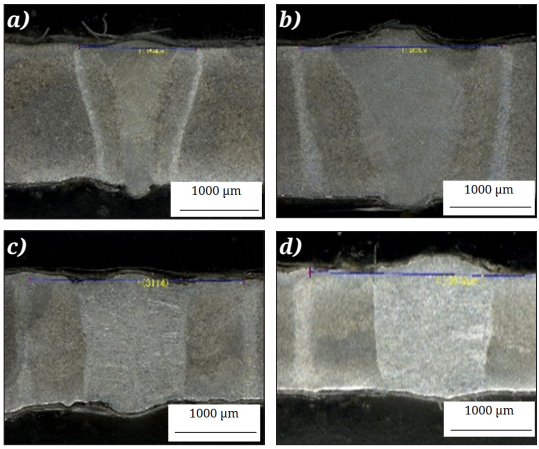

Fig. 2. *Macrographs of welds on Mn-B alloy steel samples.*
a) v = 4100 mm/min, b) v = 2500 mm/min,
c) v = 1300 mm/min, d) v = 1050 mm/min

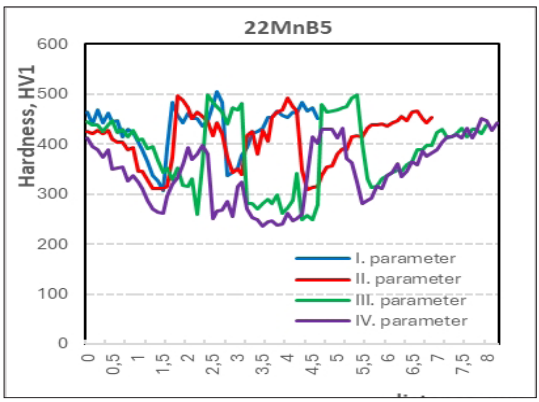

Fig. 3. *The effect of welding speed on hardness changes in the weld-metal and its surroundings in the case of Mn-B alloyed steel.*

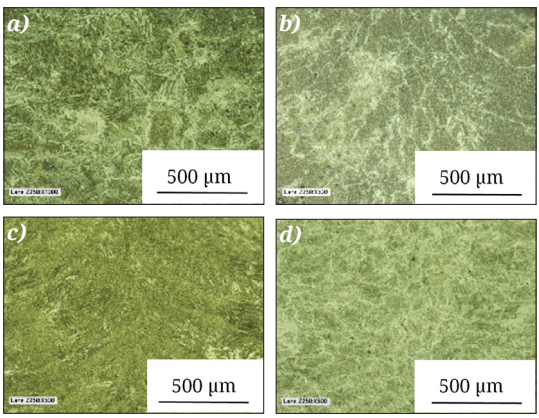

Fig. 4. *The microstructure of weld-metal in the case.*
a) v = 4100 mm/min,
b) v = 2500 mm/min, c) v = 1300 mm/min,
d) v = 1050 mm/min

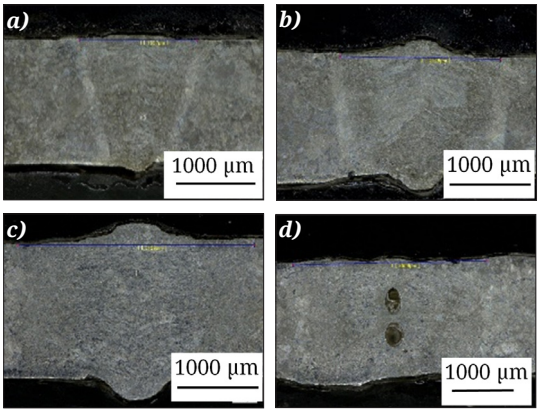

Fig. 5. *Macrographs of welds on S235JR steel samples a) v = 4100 mm/min, b) v = 2500 mm/min, c) v = 1300 mm/min, d) v = 1050 mm/min*

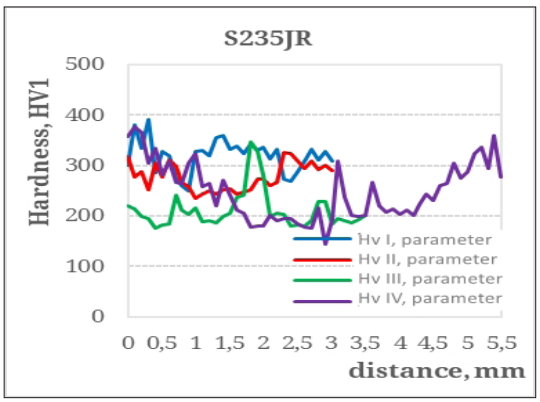

Fig. 6. *The effect of welding speed on hardness changes in the weld-metal and its sur-roundings in the case of S235JR steel.*

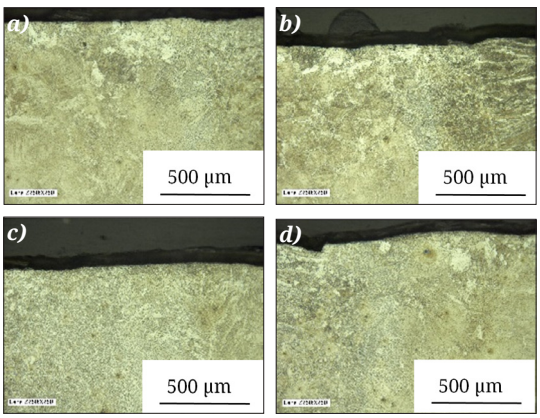

Fig. 7. *Heat affected zones after laser welding of martensitic S235JR sheet at different welding speed a) v = 4100 mm/min, b) v = 2500 mm/min, c) v = 1300 mm/min, d) v = 1050 mm/min.*

When we used a welding speed of 1050 mm/min, we found soft weld-metal, with a hardness below 200 HV1 over a width of more than 2 mm, gradually increasing towards the base material. Using this welding speed, large porosities were observed, as can be seen on **Fig. 5** d). The formation of porosity can be attributed to the excessively low welding speed. There are data in the literature indicating that in laser welding, if the welding speed is not high enough, a plasma channel begins to form at the start of welding and then deepens. Subsequently, due to the flow conditions of the melt, the plasma channel collapses, the gas inclusion remains in the material, and then the plasma channel begins to form again **[19]**.

The hardnesses that develops in the heat-affected zone of the welds can be explained by changes in the microstructure, which are presented in **Fig. 7**.

4. Conclusions

In the present experiments, laser welding of two low-carbon steel grades was investigated, which were previously martensitically hardened

During laser welding of low-carbon lath martensitic steels, no cracks formed in the weld or its heat-affected zone, even in Mn-B-alloyed steel, where the hardness approached 500 HV1 in some places when high welding speeds were used.

It was found that a welding speed of 4100 mm/min resulted in complete weld penetration for the sheet thicknesses used in the automotive industry, with the hardness of the weld metal approaching that of heat-treated martensite, with a narrow softening heat-affected zone in both steel grades tested. In the case of Mn- and B-alloyed materials, the weld metal softened at a welding speed of 1300 mm/min, while in the case of S235JR material, even a welding speed of 2500 mm/min caused softening.

A welding speed of 1050 mm/min is too low, and large porosities relative to the weld were also formed in the S235JR steel plate.

References

[1] Krauss G.: *Principles of Heat Treatment of Steel.* ASM international, USA, Materials Park, Ohio, 1980. 52.

[2] Stormvinter A., Peter Hedström P., Borgenstam A.: *Investigation of Lath and Plate Martensite in a Carbon Steel.* Solid State Phenomena, 172–174. (2011) 61–66. ISSN 1012-0394. https://doi.org/10.4028/www.scientific.net/SSP.172-174.61

[3] Galindo-Nava E. I., Rivera-Díaz-del-Castillo P. E. J.: *Understanding the factors controlling the hardness in martensitic steels.* Scripta Materialia, 110.

(2016) 96–100. ISSN 1359-6462. https://doi.org/10.1016/j.scriptamat.2015.08.010.

[4] Sandvik B. P. J., Wayman C. M.: *Crystallography and substructure of lath martensite formed in carbon steels.* Metallography, 16/2. (1983) 199–227. https://doi.org/10.1016/0026-0800(83)90005-8

[5] Kelly P. M.: *Crystallography of lath martensite in steels. Materials Transactions*. JIM (Japan), 33/3. (1992) 235–242. https://doi.org/10.2320/matertrans1989.33.235

[6] Ball J. M., Carstensen C.: *Nonclassical austenite-martensite interfaces*. Le Journal de Physique, IV. 7(C5), (1997) 35–40. https://doi.org/10.1051/jp4:1997505

[7] Morito S., Tanaka H., Konishi R., Furuhara T. & Maki T.: *The morphology and crystallography of lath martensite in Fe-C alloys.* Acta Materialia, 51. (2003) 1789–1799. https://doi.org/10.1016/S1359-6454(02)00577-3

[8] Morito S., Adachi Y., Ohba T.: *Morphology and Crystallography of Sub-Blocks*. Materials Transactions, 50/8. (2009) 1919–1923.

[9] Fábián E. R., Kótai Á.: *A léces martenzit viselkedése hőkezelés hatására.* Acta Materialia Transylvanica, 1/1. (2018). 26–30. https://doi.org/10.2478/amt-2018-0007

[10] Szabó P. J.: *Intenzív alakítási és hőkezelési folyamatok mikroszerkezetre gyakorolt hatásának értelmezése visszaszórt elektrondiffrakcióval.* BME 2012, MTA doktori mű.

[11] Lopez Granados N. M., Salinas Rodriguez: *A ˙EBSD Investigation on Effect of Cooling Rate on Microstructure and Transformation Textures of High Strength Hot-rolled Steel Plates*. Journal of Iron Steel Research International, 23/3. (2016) 261–269. https://link.springer.com/article/10.1016/S1006-706X(16)30043-7

[12] Morito S., Huang X., Furuhara T., Maki T., Hansen N.: *The morphology and crystallography of lath martensite in alloy steels.* Acta Materialia, 54. (2006) 5323–5331. https://doi.org/10.1016/j.actamat.2006.07.009

[13] Tisza M.: *Hot Forming of Boron Alloyed Manganese Steels*. Materials Science Forum, 885. (2017) 25–30. https://doi.org/10.4028/www.scientific.net/msf.885.25

[14] Huang J., Li L., Luo Z., Huang M., Peng Z., Gao J., Ke H., Liang Z.: *Improving the ductility of ultra-high strength lath martensite through heterogeneous carbon distribution*. Journal of Materials Research and Technology, 27/November–December (2023) 8209–8215.

[15] Autóipari alkalmazások. Újdonságok az autóipar területén. https://automo-tive.arcelor-mittal.com/tailored_blanks_home/LWB_home/LWB_hotstamping (letöltve: 2025. december 18.)

[16] Press Hardening Steel Grades, World Auto Steel. https://ahssinsights.org/metallurgy/steel-grades/phs-grades/ (letöltve: 2025. december 12.)

[17] Babu S. R., Nyyssönen T., Matias Jaskari M., Järvenpää A., Davis T. P., Pallaspur S., Kömi J., Porter D.: *Observations on the Relationship between Crystal Orientation and the Level of Auto-Tempering in an As-Quenched Martensitic Steel.* Metals 9/12. (2019) 1255. https://doi.org/10.3390/met9121255

[18] Bai J., Jin S., Liang Ch., Li X., You Z., Zhao Y., Liu L., Sha G.: *Microstructural origins for quench cracking of a boron steel: Boron distribution.* Materials Characterization, 190. (2022) 112022. ISSN 1044-5803. https://doi.org/10.1016/j.matchar.2022.112022

[19] Runqi Lina Hui, Wangb Fenggui, Lua Joshua, Solomonb Blair E. Carlsonb: *Numerical study of keyhole dynamics and keyhole-induced porosity formation in remote laser welding of Al alloys.* International Journal of Heat and Mass Transfer, 108. Part A, May (2017) 244–256.